Journal of Molecular Catalysis A: Chemical 394 (2014) 232–243

Contents lists available at ScienceDirect

Journal of Molecular Catalysis A: Chemical

journal homepage: www.elsevier.com/locate/molcata

Mesoporous alumina sulphuric acid: A novel and efficient catalyst for on-water synthesis of functionalized 1,4-dihydropyridine derivatives via β-enaminones

Nayeem Ahmed, Zeba N. Siddiqui*

Department of Chemistry, Aligarh Muslim University, Aligarh 202 002, India

ARTICLE INFO

Article history:
Received 10 June 2014
Received in revised form 9 July 2014
Accepted 10 July 2014
Available online 19 July 2014

Keywords:
On-water
Dihydropyridines
Mesoporous alumina sulphuric acid
Heterogeneous catalyst

ABSTRACT

A simple, efficient and environmentally benign on-water protocol for the synthesis of novel 1,4-dihydropyridine derivatives via pseudo four component addition and cyclization sequence using mesoporous alumina sulphuric acid as a recyclable and heterogeneous catalyst, has been described. The catalyst showed excellent catalytic activity giving products in high yields and could be reused for seven successive catalytic cycles. The catalyst was characterized by FT-IR, XRD, FE-SEM, EDX and TG analyses. The mesoporosity of alumina was determined by BET and TEM analyses.

1. Introduction

In the light of green chemistry water is uniquely advantageous as a solvent. It is environmentally benign, non-flammable, possesses a high heat capacity, and tolerates a wide range of temperature, making it inherently safe. It also possesses the remarkable ability to catalyze chemical transformations between some insoluble organic reactants and this phenomenon, termed as "on-water" catalysis by Sharpless and co-workers, was first observed in the late 1930s but is only now being widely adopted [1–8]. Subsequent mechanistic studies have established that this behaviour results from enforced hydrophobic interactions [9] and stabilization of the activated complex by hydrogen-bond formation [10]. Sharpless's group has shown that several uni- and bimolecular reactions are greatly accelerated when carried out in vigorously stirred aqueous suspensions. These reactions include the important classes such as cycloadditions, ene reactions, Claisen rearrangements and nucleophilic substitutions [1].

Multicomponent reactions (MCRs) have become powerful tools of synthetic organic chemistry in recent years owing to exceptional synthetic efficiency, intrinsic atom economy, high selectivity, and procedural simplicity [11]. These reactions enable straightforward access to large libraries of structurally related, drug-like compounds and thereby facilitating lead generation and lead optimization in drug discovery [12]. In a true sense, these represent environmentally friendly processes by reducing the number of steps, energy consumption and waste production [13].

Nitrogen containing heterocycles are subunits found in numerous natural products and many biologically active pharmaceuticals. Among these 1,4-dihydropyridine substructures are among the most prevalent, the most famous ones certainly being the calcium agonists Felodipine, Nicardipine, Nimodipine, Nifedipine (Fig. 1) and NADPH. In addition, these compounds show other versatile biological profiles such as anticonvulsant activity, selective adenosine-A3 receptor antagonism, radioprotective activity, sirtuin activation and inhibition, antitumor, antidiabetic, or photosensitizing activities [14–16]. Conventionally, 1,4-DHPs can be synthesized via the Hantzsch reaction, reduction of pyridines, addition to pyridines or cycloadditions, etc. but the Hantzsch reaction still remains a frequently employed tactic for the synthesis of these compounds [17]. New efforts to develop structurally diverse 1,4-DHPs led to the utilization of enaminones as substrates and few reports available in literature employing L-proline/MeOH, TMSCl, TsOH/DCE, $NaAuCl_4$ and AcOH [17,18] as catalytic systems. However, these methods exhibit limited substrate tolerance and reactivity, suffer from low yields, and use of toxic solvents. Hence it is highly desirable to develop a new protocol for the synthesis of 1,4-DHPs using enaminones, which is highly efficient, environmentally benign and tolerates wide range of substrates.

---

* Corresponding author. Tel.: +91 9412653054.
E-mail addresses: siddiqui_zeba@yahoo.co.in, zns.siddiqui@gmail.com (Z.N. Siddiqui).

http://dx.doi.org/10.1016/j.molcata.2014.07.015
1381-1169/

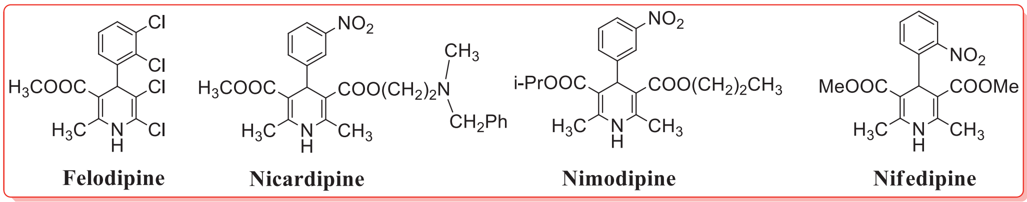

Fig. 1. Most representative biologically active 1,4-dihydropyridines.

Many industrial processes are catalyzed by strong Brønsted acid catalysts including sulfuric acid, p-toluenesulfonic acid, etc. However, such homogeneous acids are costly, require special processing in the form of neutralization, cannot be separated from homogeneous reaction mixtures and are not environmentally benign, resulting in substantial energy wastage and the production of large amounts of chemical waste. Replacing such conventional “homogeneous Brønsted acids” with recyclable solid acids is a very promising solution to this problem, and the potential of these solid acids has been extensively studied [19,20].

Keeping in view the importance of enaminones in synthesis of various heterocycles [21] herein, we report the synthesis of substituted novel 1,4-dihydropyridine derivatives via pseudo four component addition and cyclization involving β-enaminone, different aldehydes and ammonium acetate catalyzed by mesoporous alumina sulphuric acid in aqueous media. It is pertinent to mention that enaminones and related compounds possessing a nitrogen functionality and an electron-withdrawing group on adjacent alkene carbons display both the nucleophilic and the electrophilic character. This complementary electronic nature of the enaminones has led to their utilization as building blocks for the synthesis of many therapeutic agents such as antitumor, antibacterial, antimalarial, and anti-inflammatory as well as anticonvulsant agents [22–24].

2. Experimental

2.1. General

Melting points of all the synthesized compounds were taken in a Riechert Thermover instrument and are uncorrected. The IR spectra were recorded on Perkin Elmer RXI spectrometer using KBr pellets. ^{1}H NMR and ^{13}C NMR spectra were recorded on a Bruker DRX-400 spectrometer using tetramethylsilane (TMS) as an internal standard and DMSO-d_6/$CDCl_3$ as solvent. Mass spectra were recorded on Micromass Quattro II (ESI) spectrometer. Elemental analyses (C, H and N) were conducted using the Elemental vario EL III elemental analyser and their results were found to be in agreement with the calculated values. TGA data was obtained with DSC-60 Shimadzu instrument and the analysis was performed in the temperature range of 0–600 °C at a constant heating rate of 20 °C/min in the nitrogen atmosphere. X-ray diffractograms (XRD) of the catalyst were recorded in the 2θ range of 20–80° with scan rate of 4°/min on a Rigaku Minifax X-ray diffractometer with Ni-filtered Cu Kα radiation at a wavelength of 1.54060 Å. The FE-SEM and EDX characterization of the catalyst was performed on QUANTA 200 FEG from FEI Netherlands. TEM analysis was performed on JEM-2100 F Model (ACC. Voltage: 200 kV) electron microscope. BET surface area of the sample was measured from the nitrogen adsorption/desorption isotherms obtained by using a Quantachrome Autosorb 1C BET analyzer at 77 K temperature [25]. Prior to gas adsorption, the sample was degassed for 3 h at 423 K. All reagents were purchased from Merck, Aldrich and were used without further purification. The purity of compounds was checked by thin layer chromatography (TLC) on glass plates coated with silica gel G254 (E. Merck) using chloroform–methanol (3:1) mixture as mobile phase and visualized by iodine vapours and alcoholic ferric chloride. Enaminones were synthesized by reported procedure [26].

2.2. Preparation of mesoporous alumina

In a typical synthesis, N-cetyl-N,N,N-trimethylammonium bromide (CTAB) (0.2 mmol), $Al_2(SO_4)_3 \cdot 18H_2O$ (1 mmol), $CO(NH_2)_2$ (4 mmol), and sodium tartrate (0.7 mmol) were dissolved in distilled water to form a clear solution (36 mL) under vigorous stirring for 0.5 h. The solution was placed in an autoclave with a Teflon liner and was maintained at 165 °C for 8 h. The autoclave was then allowed to cool and the white precipitate obtained was collected, washed thoroughly with distilled water and then dried at 80 °C for 12 h. The sample was then calcined at 550 °C for 3 h to remove the template [27].

2.3. Preparation of mesoporous alumina supported sulphuric acid

A 0.5 L suction flask was equipped with a constant pressure dropping funnel. The gas outlet was connected to a vacuum system through an adsorbing solution of alkali trap. Mesoporous alumina (1 g) was added into the flask and stirred for 10 min in dry CH_2Cl_2 (20 mL). Chlorosulfonic acid (1 mL) was added drop wise over a period of 30 min at room temperature. After complete addition of chlorosulfonic acid, the reaction mixture was stirred for 90 min, while the residual HCl was eliminated by suction. The mesoporous alumina sulphuric acid obtained as solid, was separated from the reaction mixture by filtration and washed several times with dried CH_2Cl_2, ethanol. Finally the catalyst was dried at 120 °C for three hours.

2.4. Determination of H^+ ion concentration of mesoporous alumina sulphuric acid

H^+ ion concentration of the catalyst was determined by neutralization titration analysis. 100 mg of catalyst was stirred in 20 mL of 0.1 N NaOH solution for 30 min in an Erlenmeyer flask. The excess amount of base was then neutralized by the addition of 0.1 N HCl solution to the equivalence point of titration.

2.5. General procedure for “On water” synthesis of dihydropyridines

A mixture of β-enaminone (10 mmol), aldehyde (5 mmol), ammonium acetate (7 mmol) and catalyst (250 mg) in 10 mL water was refluxed in an oil bath for appropriate period of time (Table 4). After completion of reaction (monitored by TLC), the reaction mixture was allowed to cool and added ethyl acetate to extract the product. The catalyst as insoluble solid was separated by filtration, washed with ethyl acetate (3× 10 mL) and reused for further catalytic cycles. The filtrate was washed with water (3× 10 mL), dried over anhydrous Na_2SO_4 and evaporated under reduced pressure.

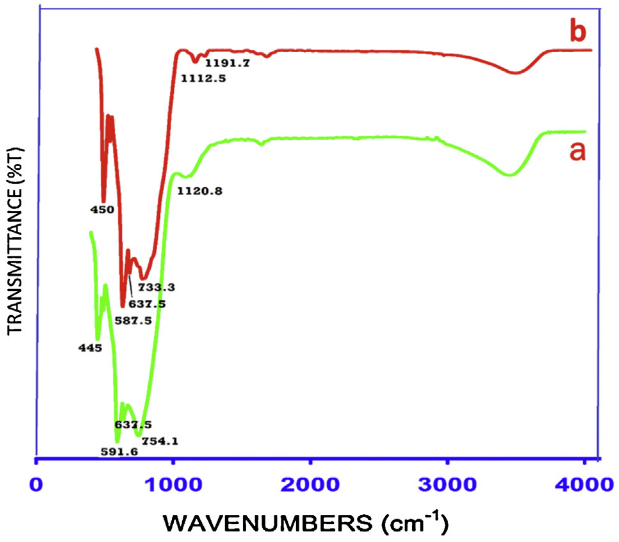

Fig. 2. FT-IR spectra of (a) mesoporous alumina sulphuric acid and (b) mesoporous alumina.

The crude product was recrystallized from suitable solvent (ethanol or DMSO) to afford pure product.

3. Results and discussion

γ-Al_2O_3 nanoparticles owing to an inherently porous morphology with an ultrafine crystallite size and a consistently large surface area, combined with high thermal and chemical stabilities, are among the most important catalytic nanomaterials used as a support in heterogeneous catalysis. Its large surface area and open porosity enable a high dispersion of catalyst which guarantees efficient contact of the catalyst with the reactant molecules. Mesoporous γ-Al_2O_3 nanoparticles were prepared by hydrothermal method using aluminium sulphate as precursor. The sulfonic acid functionalized alumina catalyst was prepared by reaction of mesoporous alumina with chlorosulfonic acid (Scheme 1). The amount of acid groups due to functionalization of the surface hydroxyl groups of alumina was calculated by using neutralization titration method and found to be 3.6 mequiv./g.

3.1. *FT-IR analysis*

The FT-IR spectra of the synthesized nanoparticles with and without SO_3H loading are shown in Fig. 2. In the spectra of alumina, transmission band obtained around 3400 cm^{-1} is characteristic of stretching vibrations of OH groups present on the surface of alumina. The band at 500–1000 cm^{-1} can be attributed to the bending and stretching vibrations of Al—O group [28]. In the spectra of functionalized alumina, the broad band at 1120 cm^{-1} is attributed to asymmetric and symmetric stretching modes of O=S=O group whereas the S—O stretching band obtained at 600–700 cm^{-1} has been merged with the bending and stretching bands of Al—O group [29]. The functionalization of sulfonic groups on the surface of alumina also lead to decrease in the intensity of bands centred around 500–1000 cm^{-1}. The IR spectra thus confirm that the sulfonic groups functionalized the surface of the alumina nanoparticles.

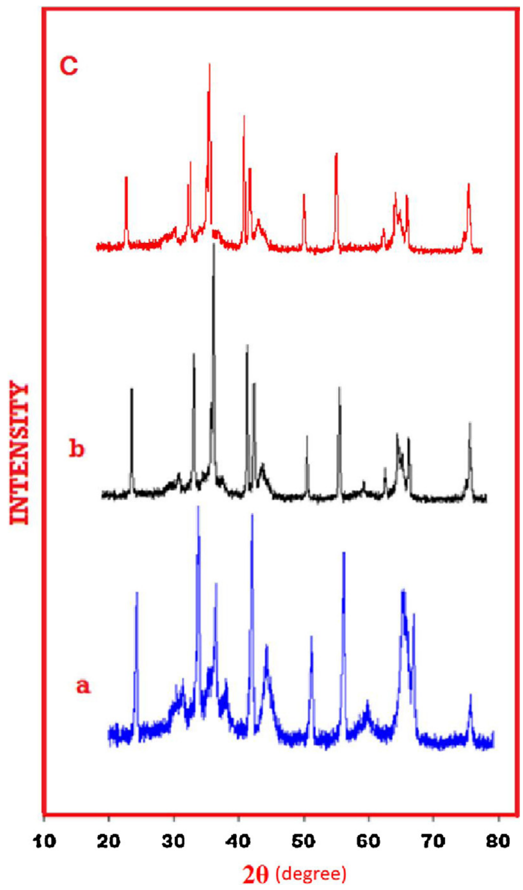

Fig. 3. (a) Powder XRD pattern of mesoporous alumina, (b) XRD pattern of fresh mesoporous alumina sulphuric acid and (c) XRD pattern of the catalyst after seven catalytic cycles.

3.2. *XRD analysis*

The formation of alumina and meso-Al-OSO_3H was observed by XRD analysis (Fig. 3). The XRD pattern of alumina shows diffraction peaks corresponding to γ-Al_2O_3 (broad peaks around 30°, 45°, 60° and 65°) and α-Al_2O_3 (sharp peaks around 25°, 35°, 40°, 50° and 55°) phases [30]. The XRD spectrum of meso-Al-OSO_3H, however showed some extra peaks and some slight changes in the nature of

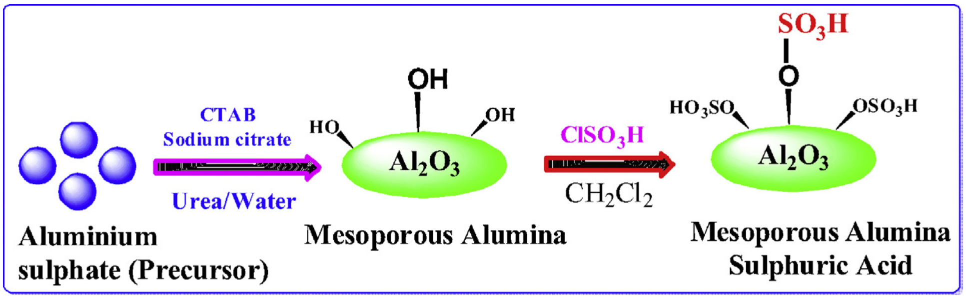

Scheme 1. Schematic representation of the synthesis of the catalyst.

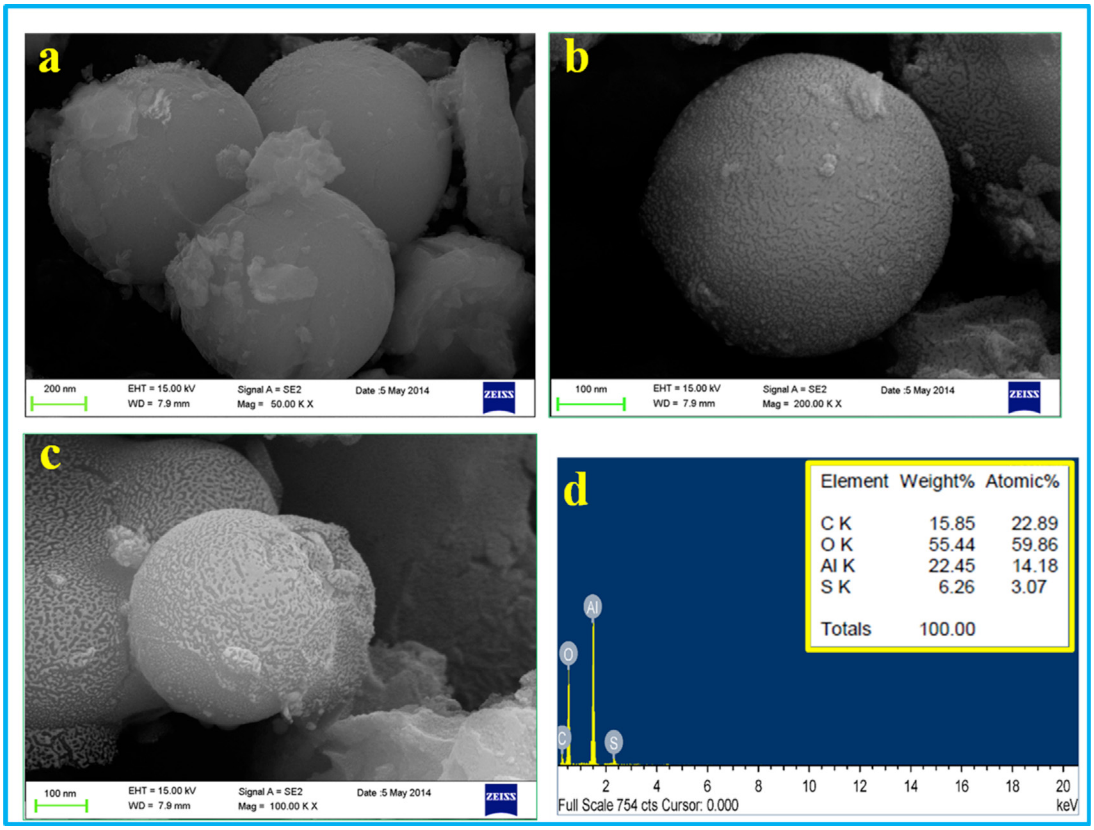

Fig. 4. FE-SEM images (a and b) of freshly synthesized mesoporous alumina at different magnifications (c) of mesoporous alumina sulphuric acid and (d) EDX analysis of mesoporous alumina sulphuric acid showing the presence of S in addition to Al and O.

peaks which may be due to the presence of sulfonic acid groups on the surface of alumina.

3.3. FE-SEM and EDX analysis

FE-SEM images (Fig. 4a and b) showed the spherical shape of the synthesized mesoporous alumina nanoparticles and the size of the particles was found to be in the range of 400 nm. Fig. 4c showed the surface of alumina after functionalization with sulfonic acid groups. It can be observed that there is no change in the shape of alumina particles after being functionalized with sulfonic acid and the surface morphology is also retained. The successful functionalization was further confirmed by EDX analysis (Fig. 4d) which showed the presence of S in addition to Al and O.

3.4. BET and TEM analyses

The mesoporous structure of γ-alumina was confirmed by N_2 adsorption/desorption isotherms (Fig. 5a). The sample showed the presence of type IV isotherm (definition by IUPAC) [31] which is a characteristic of mesoporous material. The surface area of the sample was calculated by Brunauer–Emmett–Teller (BET) method which employed nitrogen adsorption at different pressures at the liquid nitrogen temperature (77 K) and was found to be 529.54 m^2/g. The pore size distributions were also obtained from these adsorption isotherms by employing Barrett–Joyner–Halenda (BJH) method and the pore volume and average pore size obtained were 0.5 cm^3/g and 5.5 nm respectively (Fig. 5b). The less broadening in the pore width peak denotes the presence of uniform size pores. TEM images (Fig. 6) of the synthesized alumina particles were obtained in order to further confirm their mesoporous structure. The images showed wormhole-like porous structure of the molecules with uniform pore size distribution. All these analyses proved the mesoporous nature of synthesized alumina nanoparticles.

3.5. TG analysis

The thermal stability of the catalyst and successful incorporation of sulphuric acid groups on mesoporous alumina surface was observed by TG analysis (Fig. 7a and b). Fig. 7b shows the TGA curve of mesoporous alumina. The curve shows a weight loss of 8.97% up to 180 °C which is due to evaporation of moisture trapped in alumina framework. The TG curve then does not show any further weight loss up to 600 °C. In the TG curve of mesoporous alumina sulphuric acid (Fig. 7a), the first weight loss below 100 °C (13.7% up to 200 °C) is due to the removal of solvent and water molecules trapped in alumina matrix. Another weight loss of 8.9% beginning from 300 °C up to 600 °C can be attributed to the decomposition of sulfonic acid groups from the mesoporous alumina surface. The TG curve, thus, shows successful incorporation of sulfonic acid groups on the alumina surface.

3.6. Optimization of reaction conditions

3.6.1. Optimization of catalysts

Keeping in view the environmental concerns as well as the vast utility and scope of reactions carried out in water, we chose water as the preferred solvent for our reaction. In order to find right catalyst for our reaction we first tried the reaction in the absence of any catalyst. The reaction failed to produce any yield demonstrating the need of a catalyst. AcOH and H_2SO_4 catalyzed reactions gave unsatisfactory yields (Table 1, entries 1 and 2). We then used heterogenized sulphuric acid catalysts and the yields of the product

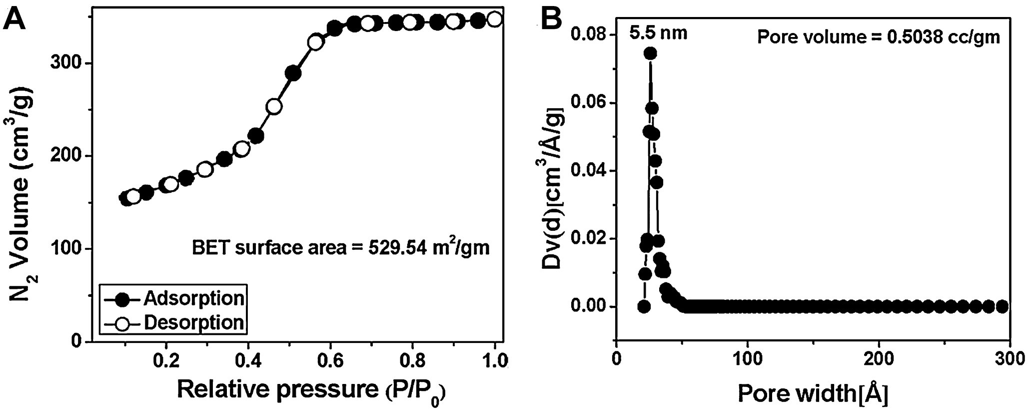

Fig. 5. (a) Nitrogen adsorption isotherm and (b) pore size distribution of mesoporous alumina.

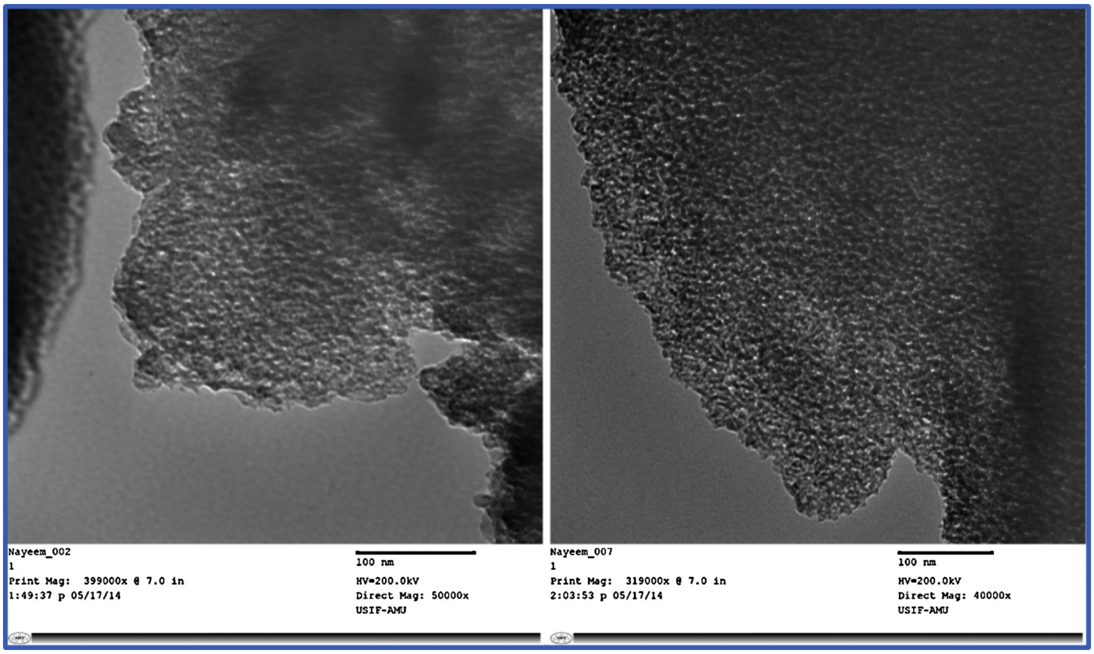

Fig. 6. TEM images of mesoporous alumina showing uniform pore distribution.

started to improve. Among silica, zirconia and alumina supported sulphuric acid, alumina sulphuric acid catalyzed reaction showed better results (Table 1, entries 3–5). Organic polymers supported sulphuric acid catalysts also showed inferior results in comparison to alumina sulphuric acid (Table 1, entries 8 and 9). We then tried the reaction using sulphuric acid supported on silica and alumina nanoparticles (Table 1, entries 10 and 11). With the introduction of nanoparticles as supports, the yields of the product increased substantially with decrease in time taken for completion of the reaction. In order to further optimize the catalyst, the reaction was performed in presence of Lewis acid catalysts like ZnO, MgO and meso-Al_2O_3 (Table 1, entries 14–16) also. The results obtained were unsatisfactory as low yield of product was obtained after prolonged reaction times. The results obtained showed that the nano-alumina sulphuric acid was the most efficient catalyst for this reaction. The higher activity shown by alumina supported acid may be due to fine dispersion of sulfonic acid groups on the surface of alumina as compared to other supports. As a simplistic manner to further improve this catalytic system, we used mesoporous alumina as a support for functionalizing sulphuric acid, the results obtained were highly encouraging and also, as can be seen, lesser amount of the catalyst was needed to catalyze this reaction efficiently (Table 1, entry 13). This higher activity shown by mesoporous alumina sulphuric acid is due to the porous structure generating a very high surface area which in turn leads to higher number of sites being available for functionalization with sulfonic acid group.

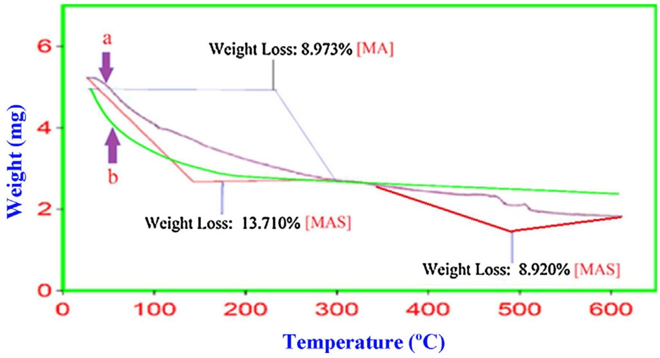

Fig. 7. TG analysis (a) of mesoporous alumina sulphuric acid [MAS] and (b) of mesoporous alumina [MA].

Table 1
Effect of various reaction media for the model reaction.[a]

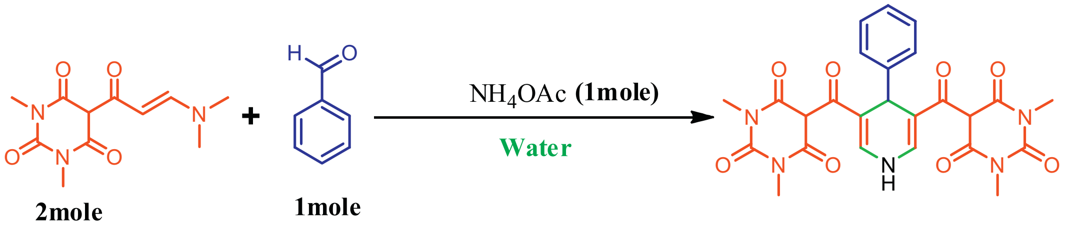

Entry	Catalyst	Condition	Time[b]	Yield[c] (%)
1	AcOH (10 mol%)	Water/reflux	7.0 h	61
2	H_2SO_4 (10 mol%)	Water/reflux	6.2 h	58
3[d]	H_2SO_4–SiO_2 (200 mg)	Water/reflux	3.5 h	72
4[d]	H_2SO_4–ZrO_2 (200 mg)	Water/reflux	4.2 h	62
5[d]	H_2SO_4–Al_2O_3 (200 mg)	Water/reflux	3.0 h	75
6[d]	NH_2SO_3H–SiO_2 (200 mg)	Water/reflux	3.4 h	66
7[d]	TsOH–SiO_2 (200 mg)	Water/reflux	4.1 h	64
8[d]	H_2SO_4–cellulose (200 mg)	Water/reflux	5.8 h	59
9[d]	H_2SO_4–xanthan (200 mg)	Water/reflux	5.2 h	61
10[d]	H_2SO_4–nanoSiO_2 (100 mg)	Water/reflux	2.2 h	78
11	H_2SO_4-nanoAl_2O_3 (100 mg)	Water/reflux	1.8 h	81
12	H_2SO_4–meso-Al_2O_3 (100 mg)	Water/reflux	45 min	90
13	H_2SO_4–meso-Al_2O_3 (50 mg)	Water/reflux	45 min	90
14	ZnO (10 mol%)	Water/reflux	8.4 h	54
15	MgO (10 mol%)	Water/reflux	9.5 h	48
16	Meso-Al_2O_3 (10 mol%)	Water/reflux	12.5 h	29

[a] Reaction of enaminone (**1b**) (2 mmol), benzaldehyde (**2a**) (1 mmol) and ammonium acetate (1 mmol) in the presence of different catalysts in water (10 mL) at reflux temperature.
[b] Reaction progress monitored by TLC.
[c] Isolated yield.
[d] The catalysts prepared by reported procedures [20].

3.6.2. *Effect of solvents/hydrophobic effect*

In order to establish water as a preferred solvent, the model reaction was studied using different solvents (Table 2). Using AcOH as a solvent the reaction gave only moderate yield of the product (Table 2, entry 2). Using ethanol and methanol as solvents, again unsatisfactory yield of product was obtained (Table 2, entries 3 and 4). In chloroform the reaction did not reach to completion (Table 2, entry 5). DMF as a solvent again showed unsatisfactory results (Table 2, entry 6). Using water as a solvent the reaction showed excellent results in short span of time (Table 2, entry 7). This enhanced reactivity can be attributed to the strong hydrogen bond interaction at the organic/water interface, which stabilizes the reaction intermediates and enhances the rate of reaction [10]. To further understand this impressive rate enhancement for on-water reactions, firstly, we performed the reaction under neat conditions (Table 2, entry 1), the reaction completed in 1.5 h with 77% product yield. We then performed experiments for the reaction by using different concentrations of various solvents with water. Mixing of 0.5 mL of ethanol to the water containing the reaction mixture showed no effect. Addition of further 1–2 mL of ethanol again did not showed any remarkable effect (Table 2, entries 8 and 9). Addition of 3–4 mL of ethanol turned the reaction mixture homogeneous, and then the rate of reaction decreased considerably (Table 2, entry 10). We then tried this experiment with addition of MeOH to the reaction mixture and found similar results. Upon examining the results we found that the large rate enhancements occurred if the reaction was conducted in heterogeneous conditions than in homogeneous aqueous solution and hydrophobic effects acted prominently as neat reaction was not as faster as reaction using water. These studies established the supremacy of water as a solvent for this reaction.

3.6.3. *Catalyst loading*

In order to optimize the amount of catalyst for obtaining maximum yield in lesser amount of time, effect of the catalyst loading on the model reaction was studied. It was found that when the catalyst amount was increased from 0.03 g to 0.05 g the yield of the product increased significantly from 76% to 90%. With further increase to 0.1 g the time taken and yield obtained did not change. Further increase in the catalyst concentration decreased the yields mainly due to the formation of some side products (Table 3).

3.6.4. *Catalytic reaction*

With these encouraging results in hand, we turned to explore the scope of the reaction using different aromatic aldehydes **(2a–g)**, enaminones **(1a, 1b)** and ammonium acetate as substrates under the optimized reaction conditions (Table 4). It was observed that the aromatic aldehydes with electron donating as well as electron withdrawing groups reacted successfully to furnish the final products **(3a–n)** in good yields (Scheme 2). However, the electron donating groups in aldehydes caused low reactivity and increased time period for completion of the reaction due to deactivating effects. In order to further prove the generality of our procedure, we also used alicyclic and aliphatic aldehydes (Table 4, entries 6, 7, 13 and 14) in the reaction and it was found that the reaction occurred with high efficiency and good yield of products was obtained. The structures of the final products were well characterized by using spectral (IR, ^1H, ^{13}C NMR and ESI-MS) and elemental analysis data. The I.R. Spectrum of **3h** showed broad peak at 3431 cm^{-1} which was due to stretching frequency of NH group. Two C=O groups connected to dihydropyridine ring showed absorption band at 1731 cm^{-1} and six C=O groups of two pyrimidinetrione moieties showed sharp absorption band at 1672 cm^{-1}. The absorption band at 1604 cm^{-1} was assigned to C=C stretching. The ^1H NMR Spectrum showed a broad singlet at δ10.28 ppm which was assigned to the NH proton of dihydropyridine ring. The five protons of aromatic region showed a multiplet in the range of δ 7.4–7.8 and the two hydrogen atoms present in dihydropyridine ring gave a singlet at δ 7.25 ppm. Another singlet at δ 5.29 confirmed the formation of dihydropyridine ring. ^{13}C NMR showed signals at δ 184.63, 172.11

Table 2
Effect of different solvents on the model reaction.[a]

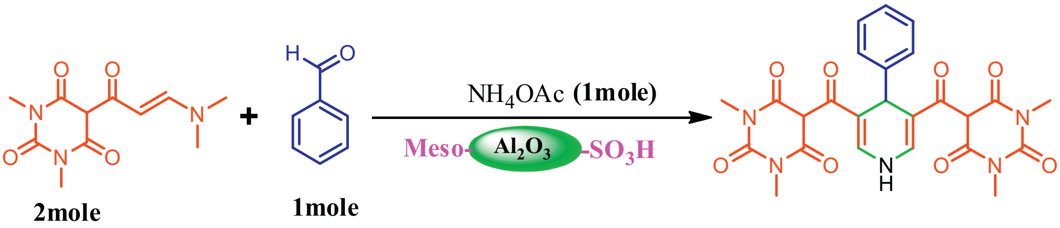

Entry	Solvent	Time[b]	Yield[c] (%)
1	Neat	1.5 h	77
2	Acetic acid (5 mL)	4 h	56
3	Methanol (5 mL)	5 h	53
4	Ethanol (5 mL)	5 h	61
5	Chloroform	5 h	Incomplete reaction
6	DMF	3 h	48
7	Water (5 mL)	45 min	90
8	Water (5 mL)/ethanol (1 mL)	45 min	88
9	Water (5 mL)/ethanol (2 mL)	50 min	86
10	Water (5 mL)/ethanol (3 mL)	3.5 h	73

[a] Reaction of enaminone (**1b**) (2 mmol), benzaldehyde (**2a**) (1 mmol) and ammonium acetate (1 mmol) in presence of mesoporous alumina sulphuric acid (0.05 g) in different solvents.
[b] Reaction progress was monitored by TLC.
[c] Isolated yield.

Table 3
Effect of catalyst loading on the model reaction.[a]

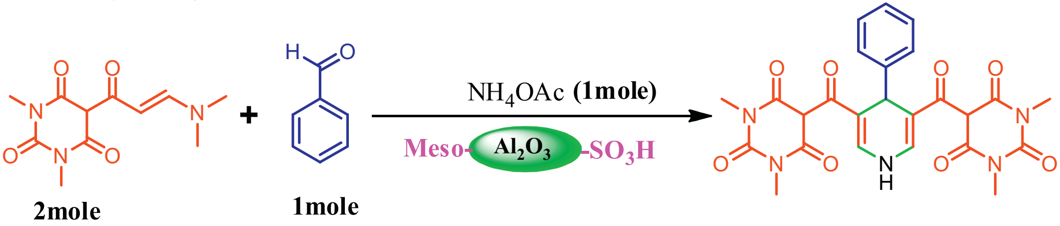

Entry	Catalyst loading (g)	Time (min)[b]	Yield[c] (%)
1	0.03	63	76
2	0.05	45	90
3	0.10	45	90
4	0.15	45	88
5	0.20	45	86

[a] Reaction of enaminone (**1b**) (2 mmol), benzaldehyde (**2a**) (1 mmol) and ammonium acetate (1 mmol) in presence of different loadings of mesoporous alumina sulphuric acid in 10 mL water at reflux temperature.
[b] Reaction progress was monitored by TLC.
[c] Isolated yield.

and 165.21 ppm for C-1″, C-4′, 6′ and C-2′ carbons respectively. Other peaks were present at their normal values and are provided in (supplementary information) Further structural confirmation was provided by ESI-mass spectrum which showed the molecular ion peak as the base peak at m/z 522.1 (M^{+}+1).

3.6.5. Reaction mechanism

The plausible mechanism is proposed in Scheme 3. First the aldehyde group of **2a** is activated by the catalyst after which it undergoes nucleophilic addition of double bond of enaminone **1b** to form **4**. Intermediate **6** then undergoes benzylic

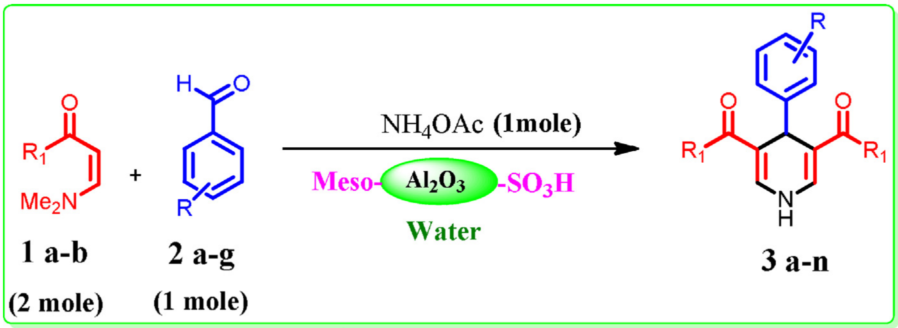

Scheme 2. General scheme for the synthesis of dihydropyridines.

Table 4
Synthesis of dihydropyridines[a].

Entry	Enaminone	Aldehyde	Product	Time (min)[b]	Yield (%)[c]
1	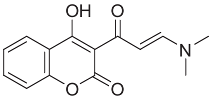 **1a**	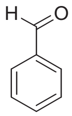 **2a**	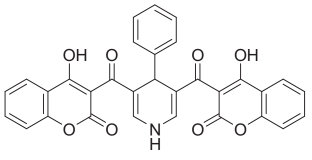 **3a**	53	89
2	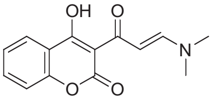 **1a**	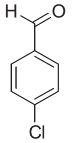 **2b**	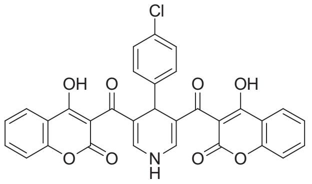 **3b**	51	86
3	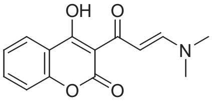 **1a**	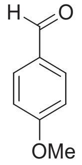 **2c**	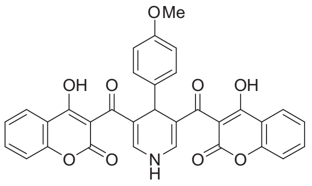 **3c**	57	85
4	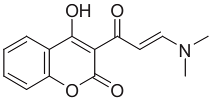 **1a**	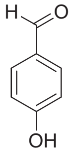 **2d**	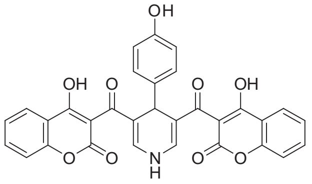 **3d**	51	87
5	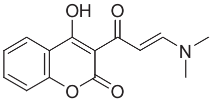 **1a**	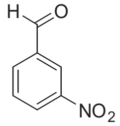 **2e**	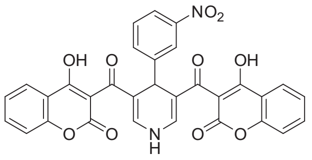 **3e**	50	83
6	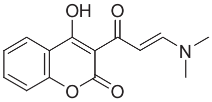 **1a**	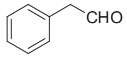 **2f**	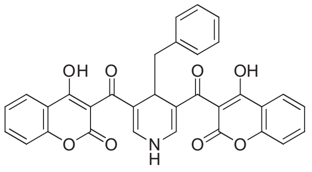 **3f**	65	84
7	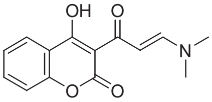 **1a**	 **2g**	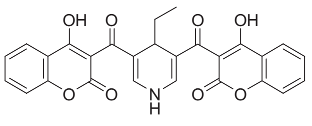 **3g**	68	81
8	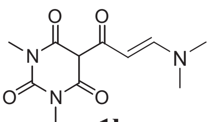 **1b**	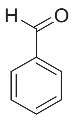 **2a**	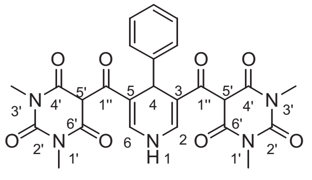 **3h**	45	90

Table 4 (*Continued*)

Entry	Enaminone	Aldehyde	Product	Time (min)[b]	Yield (%)[c]
9	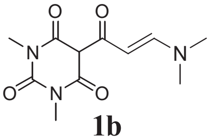 **1b**	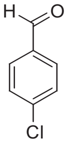 **2b**	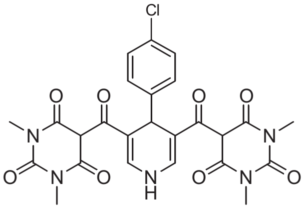 **3i**	43	89
10	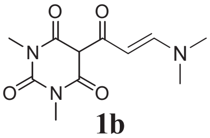 **1b**	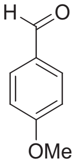 **2c**	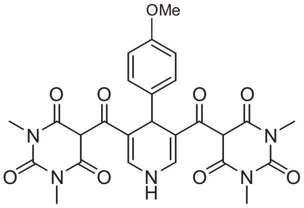 **3j**	48	87
11	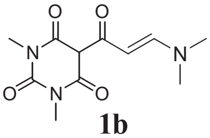 **1b**	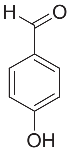 **2d**	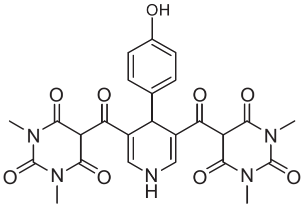 **3k**	41	90
12	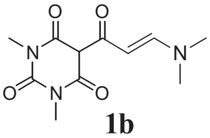 **1b**	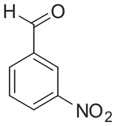 **2e**	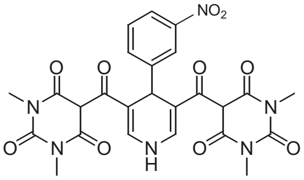 **3l**	40	86
13	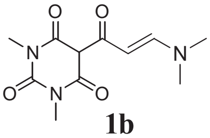 **1b**	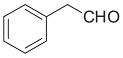 **2f**	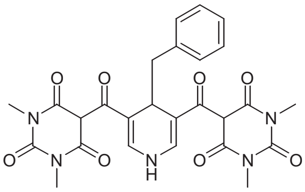 **3m**	45	85
14	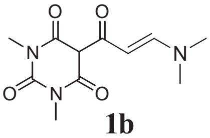 **1b**	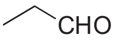 **2g**	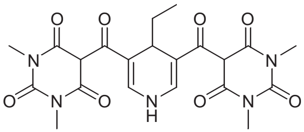 **3n**	52	82

[a] Reaction of enaminones (**1a–b**) (2 mmol), different aldehydes (**2a–g**) (1 mmol) and ammonium acetate (1 mmol) in presence of mesoporous alumina sulphuric acid (0.05 g) in 10 mL water at reflux temperature.

[b] Reaction progress was monitored by TLC.

[c] Isolated yield.

substitution by another molecule of enaminone **1b** followed by loss of water molecule to generate divinylic compound **7**. This divinylic compound then undergoes Michael addition of ammonia followed by elimination of dimethyl amine to give **9**. The compound **9** then undergoes cyclization by intramolecular Michael addition of amine followed by elimination of another molecule of dimethyl amine to give the product **3h**. The catalyst could be regenerated in the last step and reused for further catalytic cycles [17].

3.7. *Hot filtration test*

In order to check any leaching of catalyst into the solution during the reaction, a hot-filtration test was performed using mesoporous

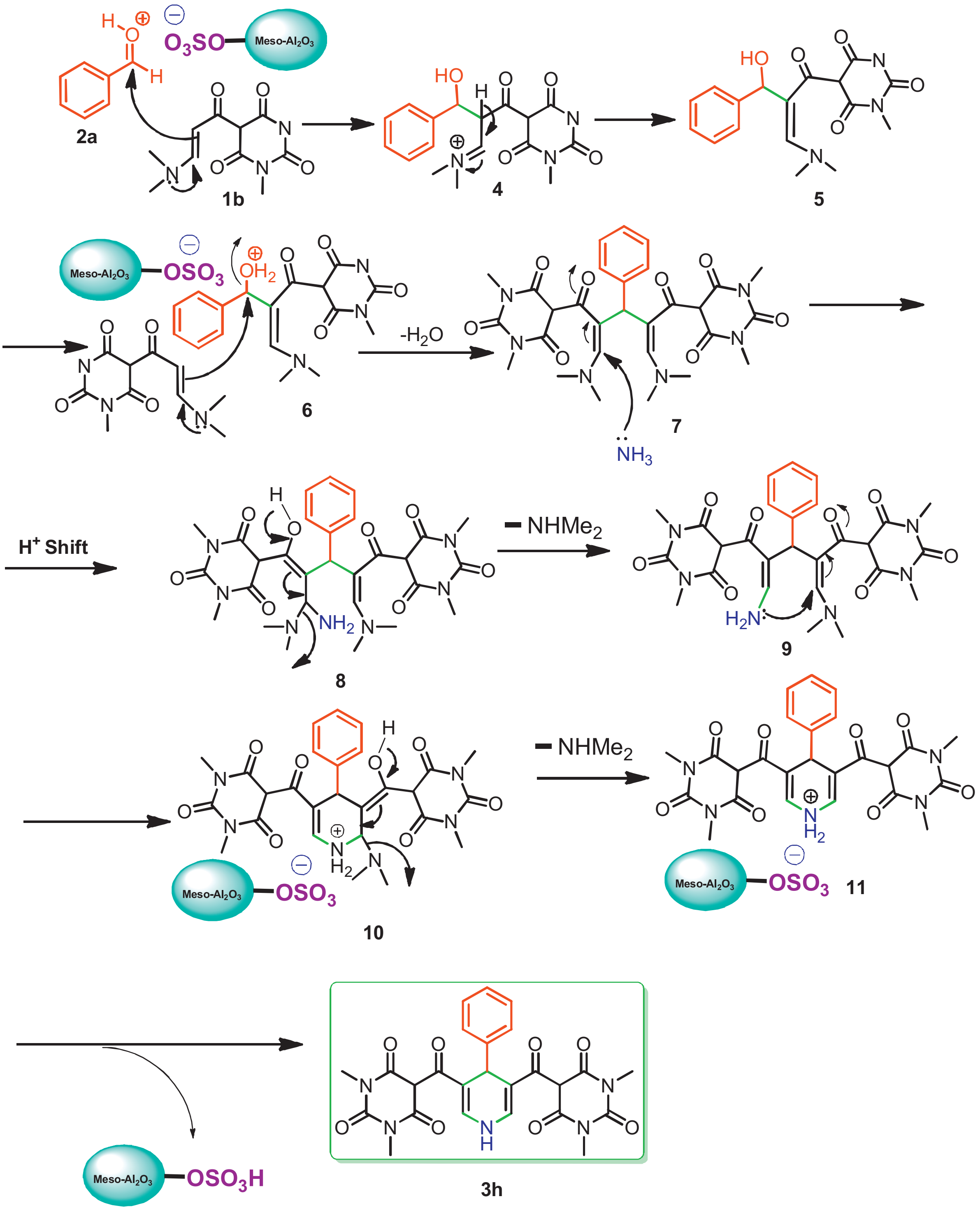

Scheme 3. Plausible reaction mechanism for the formation of 3 h.

alumina sulphuric acid as a catalyst. A mixture of β-enaminone **1b** (1 mmol), aldehyde **2a** (0.5 mmol), ammonium acetate (0.7 mmol) and catalyst (50 mg) in 5 mL ethanol was refluxed for 30 min and immediately filtered under hot reaction conditions. The reaction mixture without catalyst was then further refluxed for 6 h under the same reaction conditions. It was observed that after 6 h there was no further product formation and the reaction could not proceed to completion. This result clearly confirms the heterogeneous nature of the mesoporous catalyst and no leaching of SO_3H groups occurs during the course of reaction.

4. Catalyst recyclability

In order to explore the extent of recyclability of our catalytic system, the catalyst was recovered by filtration from the reaction mixture of enaminone **1b**, benzaldehyde and ammonium acetate in water, washed with ethanol (3× 15 mL), ethyl acetate (2× 10 mL), dried at 100 °C for 1.5 h, and reused in subsequent runs. The catalyst was found to retain its activity for a minimum of seven reaction cycles and displayed almost high catalytic performance with over 85% product yield (Fig. 8). The XRD (Fig. 3c) of the catalyst after

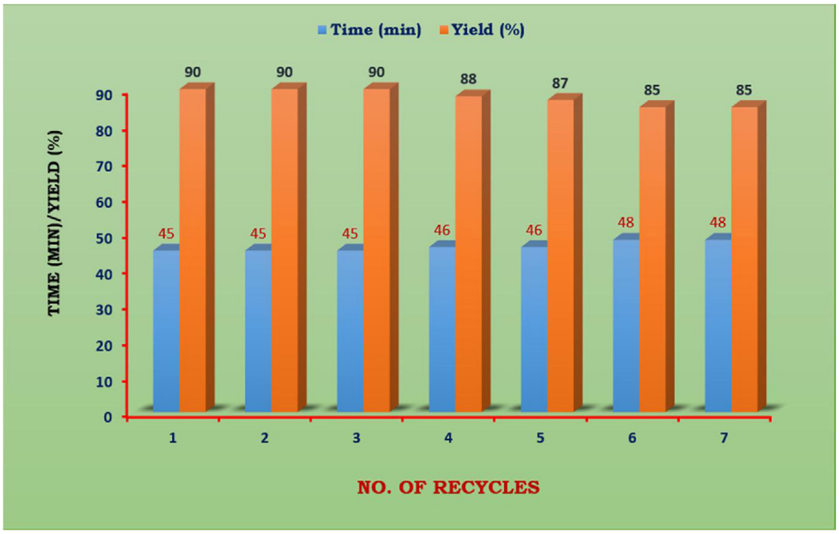

Fig. 8. Recycling data of mesoporous alumina sulphuric acid for the model reaction.

seven runs showed that the catalyst structure is preserved during its reuse.

5. Conclusion

In conclusion, an efficient, green and convenient method for the preparation of new 1,4-dihydropyridines via β-enaminones in water is reported. This new process provides an opportunity to use water and avoid environmentally harmful conventional organic solvents. In addition to aromatic aldehydes the reaction was found to be effective for both alicyclic and aliphatic aldehydes. The simple procedure for catalyst preparation, easy recovery and reusability of the catalyst are expected to contribute to its utilization for the development of benign chemical processes.

Acknowledgments

The authors are thankful to the Centre of nanotechnology, Department of Applied Physics and University Sophisticated Instrument Facility (USIF), AMU, Aligarh for providing powder XRD and TEM facilities. The authors would also like to thank SAIF Punjab University, Chandigarh for providing NMR and Mass spectra.

Appendix A. Supplementary data

Supplementary data associated with this article can be found, in the online version, at http://dx.doi.org/10.1016/j.molcata.2014.07.015.

References

[1] S. Narayan, J. Muldoon, M.G. Finn, V.V. Fokin, H.C. Kolb, K.B. Sharpless, Angew. Chem. Int. Ed. 44 (2005) 3275.
[2] V.V. Fokin, Chem. Rev. 109 (2009) 725.
[3] A.G. Coyne, Chem. Rev. 110 (2010) 6302.
[4] M.C. Pirrung, Chem. Eur. J. 12 (2006) 1312.
[5] C.J. Li, Chem. Rev. 105 (2005) 3095.
[6] C.J. Li, Chem. Rev. 93 (1993) 2023.
[7] U.M. Lindstrom, Chem. Rev. 102 (2002) 2751.
[8] S. Otto, J.B.F.N. Engberts, Org. Biomol. Chem. 1 (2003) 2809.
[9] R. Breslow, Acc. Chem. Res. 24 (1991) 159.
[10] J. Chandrasekhar, S. Shariffskul, W.L. Jorgensen, J. Phys. Chem. B 106 (2002) 8078.
[11] (a) A. Dömling, Chem. Rev. 106 (2006) 17;
(b) D.J. Ramón, M. Yus, Angew. Chem. Int. Ed. 44 (2005) 1602;
(c) A. Khazaei, M.A. Zolfigol, A.R. Moosavi-Zare, F. Abi, A. Zare, H. Kaveh, V. Khakyzadeh, M. Kazem-Rostami, A. Parhami, H. Torabi-Monfared, Tetrahedron 69 (2013) 212.
[12] P. Slobbe, E. Ruijter, R.V.A. Orru, Med. Chem. Commun. 3 (2012) 1189.
[13] (a) R.C. Cioc, E. Ruijter, R.V.A. Orru, Green Chem. 16 (2014) 2958;
(b) M.A. Zolfigol, A. Khazaei, A.R. Moosavi-Zare, A. Zare, V. Khakyzadeh, Appl. Catal. A: Gen. 400 (2011) 70;
(c) A. Khazaei, M.A. Zolfigol, A.R. Moosavi-Zare, J. Afsar, A. Zare, V. Khakyzadeh, M.H. Beyzavi, Chin. J. Catal. 34 (2013) 1936;
(d) M.A. Zolfigol, V. Khakyzadeh, A.R. Moosavi-Zare, A. Zare, S.B. Azimi, Z. Asgari, A. Hasaninejad, C. R. Chimie 15 (2012) 719.
[14] (a) R. Lavilla, J. Chem. Soc., Perkin Trans. 1 (2002) 1141;
(b) J. Moreau, J.P. Hurvois, M.D. Mbaye, J.L. Renaud, Targets Heterocycl. Syst. 13 (2009) 201.
[15] (a) C.O. Kappe, Eur. J. Med. Chem. 35 (2000) 1043;
(b) T. Godfraind, R. Miller, M. Wibo, Pharmacol. Rev. 38 (1986) 321.
[16] (a) A. Sausins, G. Duburs, Heterocycles 27 (1988) 269;
(b) M.F. Gordeev, D.V. Patel, B.P. England, S. Jonnalagadda, J.D. Combs, E.M. Gordon, Bioorg. Med. Chem. 6 (1998) 883;
(c) M.F. Gordeev, D.V. Patel, E.M. Gordon, J. Org. Chem. 61 (1996) 924.
[17] (a) D.M. Stout, A.I. Meyers, Chem. Rev. 82 (1982) 223;
(b) A. Sausins, G. Duburs, Heterocycles 27 (1988) 269;
(c) J.P. Wan, Y. Liu, RSC Advances 2 (2012) 9763.
[18] N.A. Al-Awadi, M.R. Ibrahim, M.H. Elnagdi, E. John, Y.A. Ibrahim, Beilstein J. Org. Chem. 8 (2012) 441.
[19] (a) M.J. Climent, A. Corma, S. Iborra, Chem. Rev. 111 (2011) 1072;
(b) N. Ahmed, Z.N. Siddiqui, J. Mol. Catal. A: Chem. 387 (2014) 45;
(c) Z.N. Siddiqui, K. Khan, N. Ahmed, Catal. Lett. 144 (2014) 623.
[20] (a) M.A. Zolfigol, Tetrahedron 57 (2001) 9509;
(b) B.M. Reddy, P.M. Sreekanth, P. Lakshmanan, J. Mol. Catal. A: Chem. 237 (2005) 93;
(c) A. Praminik, S. Bhar, Catal. Commun. 20 (2012) 17;
(d) Z.N. Siddiqui, N. Ahmed, Appl. Organomet. Chem. 27 (2013) 553;
(e) A. Rajack, K. Yuvaraju, C. Praveen, Y.L.N. Murthy, J. Mol. Catal. A: Chem. 370 (2013) 197;
(f) Z.N. Siddiqui, S. Tarannum, C. R. Chimie 16 (2013) 829;
(g) M.A. Zolfigol, A. Khazaei, M. Mokhlesi, F. derakhshan-panah, J. Mol. Catal. A: Chem. 370 (2013) 111;
(h) Z.N. Siddiqui, S. Tarannum, Tetrahedron Lett. 55 (2014) 2612.
[21] (a) B. Stanovnik, J. Svete, Chem. Rev. 104 (2004) 2433;
(b) A.Z.A. Elassara, A.A. El-Khairb, Tetrahedron 59 (2003) 8463;
(c) S. Muthusaravanan, C. Sasikumar, B.D. Bala, S. Perumal, Green Chem. 16 (2014) 1297;
(d) W.J. Hao, J.Q. Wang, X.P. Xu, S.L. Zhang, S.Y. Wang, S.J. Ji, J. Org. Chem. 78 (2013) 12362;
(e) Z.N. Siddiqui, N. Ahmed, F. Farooq, K. Khan, Tetrahedron Lett. 54 (2013) 3599.
[22] (a) J.E. Foster, J.M. Nicholson, R. Butcher, J.P. Stables, I.O. Edafiogho, A.M. Goodwin, M.C. Henson, C.A. Smith, K.R. Scott, Bioorg. Med. Chem. 7 (1999) 2415;
(b) J.P. Michael, C.B. Koning, G.D. Hosken, T.V. Stanbury, Tetrahedron 57 (2001) 9635.
[23] (a) D.L. Boger, T. Ishizaki, J.R.J. Wysocki, S.A. Munk, P.A. Kitos, O. Suntornwat, J. Am. Chem. Soc. 111 (1989) 6461;
(b) I.O. Edafiogho, K.V.V. Ananthalakshmi, S.B. Kombian, Bioorg. Med. Chem. 14 (2006) 5266.
[24] (a) N.D. Eddington, D.S. Cox, R.R. Roberts, J.P. Stables, C.B. Powell, K.R. Scott, Curr. Med. Chem. 7 (2000) 417;

(b) N.N. Salama, N.D. Eddington, D. Payne, T.L. Wilson, K.R. Scott, Curr. Med. Chem. 11 (2004) 2093.
[25] (a) D. Chandra, S. Mridha, D. Basak, A. Bhaumik, Chem. Commun. (2009) 2384;
(b) K. Dhara, K. Sarkar, D. Srimani, S.K. Saha, P. Chattopadhyay, A. Bhaumik, Dalton Trans. 39 (2010) 6395.
[26] Z.N. Siddiqui, F. Farooq, J. Mol. Catal. A: Chem. 363–364 (2012) 451.
[27] M.B. Yue, T. Xue, W.B. Jiao, Y.M. Wang, M.Y. He, Solid State Sci. 13 (2011) 409.
[28] (a) A.D. Cross, An Introduction to Practical IR Spectroscopy, 2nd ed., Butterworth, London, 1964;
(b) A. Teimouri, A.N. Chermahini, H. Salavati, L. Ghorbanian, J. Mol. Catal. A: Chem. 373 (2013) 38.
[29] (a) M.A. Zolfigol, A. Khazaei, M. Mokhlesi, F. Derakhshan-Panah, J. Mol. Catal. A: Chem. 370 (2013) 111;
(b) A.R. Kiasat, S. Noorizadeh, M. Ghahremani, S.J. Saghanejad, J. Mol. Struct. 1036 (2013) 216.
[30] X. Su, S. Chen, Z. Zhou, Appl. Surf. Sci. 258 (2012) 5712.
[31] S.J. Gregg, K.S.W. Sing, Adsorption Surface Area and Porosity, Academic Press, London, 1982.